STANFORD RESEARCH INSTITUTE

MENLO PARK, CALIFORNIA

Theoretical Notes
Note 49

March 1967

Final Report – Part I

PROPAGATION OF RF SURFACE WAVES ALONG A SEA-AIR INTERFACE

By: S. V. YADAVALLI G. H. PRICE

Prepared for:

AIR FORCE WEAPONS LABORATORY
RESEARCH AND TECHNOLOGY DIVISION
AIR FORCE SYSTEMS COMMAND
KIRTLAND AIR FORCE BASE, NEW MEXICO

CONTRACT AF 29(601)-7178

SRI Project 6086

Approved: W. R. VINCENT, MANAGER
COMMUNICATION LABORATORY

D. R. SCHEUCH, EXECUTIVE DIRECTOR
ELECTRONICS AND RADIO SCIENCES

ABSTRACT

Several possible effects of a rough air-sea boundary upon electromagnetic fields observed near that boundary have been examined. The calculated effects are small for surface-wave propagation above a slightly rough surface, large for surface-wave propagation above a periodic, corrugated surface, and moderate for propagation over a rough surface near a source whose dimensions are appreciably larger than the spacing between scatterers.

CONTENTS

ILLUSTRATIONS

TABLES

FOREWORD

This report, submitted 15 March 1967, describes a portion of the research Stanford Research Institute conducted during the period May 1966 through March 1967 under Air Force Contract AF 29(601)-7178 and SRI Project 6086. The Air Force Program Monitor was Captain Carl E. Baum. The report has been reviewed and approved.

I INTRODUCTION

In the study of electromagnetic phenomena, it is often necessary to make measurements near a boundary between two media that is not smooth. The surface of such a boundary can distort an electromagnetic field. The form of the distortion will depend strongly upon the ratio of surface dimensions to electromagnetic wavelength. This study considers several idealized forms of distortion, at radio frequencies from 1.0 kHz to 10 MHz, due to the roughness of a sea surface.

A sea surface is complex in that it contains a broad spectrum of random ripples. These ripples or waves vary from long-period, large-dimension swells to rapidly varying, short-dimension, wind-blown ripples. This surface is time varying and can only be described statistically. However, for most radio frequencies, particularly those considered here, the sea surface can be considered stationary, although it cannot be uniquely defined for any instant.

In studying the effects of a nonsmooth surface on electromagnetic energy, it is often convenient to make one of two simplifying assumptions. If surface dimensions are large compared to electromagnetic wavelength (high frequencies), then the surface can be considered as a collection of discrete secondary sources. If surface dimensions are small compared to wavelength, then the surface can be considered smooth, and distortion effects can be treated as an electrostatic problem. For the actual sea surface and for the frequency range of 1 kHz to 10 MHz, both these conditions exist, along with the intermediate condition that the wavelengths are similar to the surface-roughness dimensions.

To gain some insight into possible electromagnetic distortion effects caused by a rough sea surface, three mathematical models are considered:

(1) The effects of the variation in height between a point in space near the surface and the actual surface is examined by consideration of the

variation with height above the surface of an electromagnetic surface wave.

(2) The possible effects upon attenuation rate (along the surface) and decay rate (normal to the surface) are considered for the case of a propagating surface wave with wavelengths near the surface roughness dimensions.

(3) The effects of scattering upon the fields near an extended (as distinct from point) signal source are examined.

The results obtained for the mathematical models treated in this report do not define the effects of an actual rough sea surface on electromagnetic fields near such a surface. Rather, the models are highly idealized, both in the features they do consider as well as in their neglect of some possibly significant features. For example, sea spray and temperature gradients near the surface may cause field distortions, although these effects are not included in this study. Models have been chosen to demonstrate whether or not the effects considered here are significant, while the difficulties of an accurate treatment of the actual problem have been avoided.

II ELECTRICAL PROPERTIES OF SEA WATER

In the 1-kHz-to-100-MHz frequency range, the electrical properties of sea water vary considerably. The value of ε_c, the complex dielectric constant of sea water, is a function of frequency. It can be written in terms of the relative permittivity and the conductivity as

$$\varepsilon_c = \varepsilon' - i\varepsilon'' = \frac{\varepsilon}{\varepsilon_o} - i\,\frac{\sigma}{\omega\varepsilon_o} = \frac{\varepsilon}{\varepsilon_o} - i\;60\;\lambda_o\sigma$$

where

ε' is the relative permittivity of sea water (81)

σ is the conductivity of sea water (4 mhos/meter)

λ_o is the wavelength of the EM radiation in meters (corresponding to a frequency ω)

ε_o is the dielectric constant of free space (8.854×10^{-12} farads/m).

An $e^{+i\omega t}$ dependence for EM waves is assumed. The units are rationalized MKS. The desired quantity ε_c is tabulated in Table I.

From Table I it is clear that, at the frequencies of interest here, the sea may be treated as a slightly poor conductor.

Table I

COMPLEX DIELECTRIC CONSTANT OF SEA WATER

Frequency	Wavelength (EM Waves) (Meters)	ε_c (Sea Water)	Quality of Conductor
1 kHz	3×10^5	$80 - i(7.2)(10^7)$	Excellent
10 kHz	3×10^4	$80 - i(7.2)(10^6)$	Excellent
100 kHz	3×10^3	$80 - i(7.2)(10^5)$	Very good
1 MHz	300	$80 - i(7.2)(10^4)$	Good
10 MHz	30	$80 - i7200$	Fairly good
100 MHz	3	$80 - i720$	Fair

III SURFACE WAVE PROPAGATION

A. Smooth Imperfectly Conducting Surface

To arrive at a result which shows the effect of a randomly rippled surface on the propagation of a surface wave at the interface of two media, it is necessary to understand the behavior of a surface wave when there is no ripple or wave at the interface. Consider the situation shown schematically in Fig. 1. Only the TM mode (E mode) is considered, since it is assumed that no magnetic losses occur in either medium. In this case, the sea-air interface is assumed to be smooth. The interface boundary is located at x = 0, and we are interested in propagation along the z-direction.

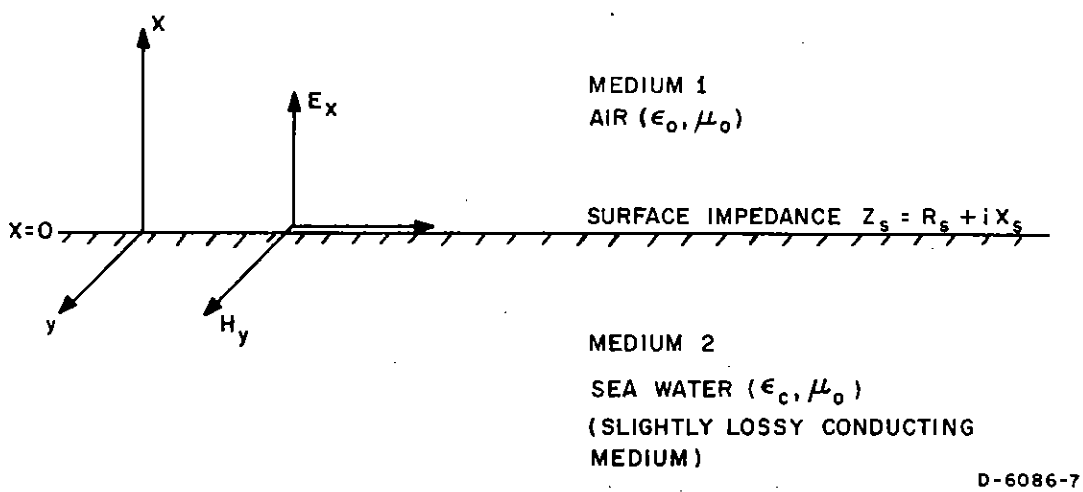

FIG. 1 SCHEMATIC OF A SMOOTH BOUNDARY

Let us now write (considering the TM mode only)

$$H_y \sim A \exp\left[i\omega t - i\beta z + i\alpha x\right] \quad , \quad x > 0 \quad . \tag{2}$$

The behavior of the field components for x > 0 is of particular interest to us. From Maxwell's equations,

$$\alpha^2 + \beta^2 = k_o^2 \qquad \left(k_o = \frac{2\pi}{\lambda_o}\right) \quad . \tag{3}$$

It can be shown that, for the surface wave to propagate, it is necessary* that

$$\alpha = \alpha' + i\alpha'' = k_o z_s = k_o R_s + ik_o X_s \tag{4}$$

and

$$\beta = \beta' - i\beta'' = \left(k_o^2 - \alpha^2\right)^{\frac{1}{2}} = k_o\left(1 + X_s^2 - R_s^2 - 2iR_s X_s\right) \quad , \tag{5}$$

where z_s is the surface impedance.

For example, when Medium 2 is a pure metal,

$$z_s = (1 + i)\left(\frac{k_o}{2\sigma z_o}\right)^{\frac{1}{2}} \tag{6}$$

and

$$z_o = 377 \text{ ohms} \quad .$$

We will assert next that Eq. (6) may be used to yield reasonable answers in our case, at least at frequencies below 10 MHz. It then follows that

$$\alpha \approx k_o(1 + i)\left(\frac{k_o}{2\sigma z_o}\right)^{\frac{1}{2}} \tag{7}$$

---

*If the wave impedance (E_z/H_y) in Medium 1 is denoted by z_1 then $z_1 = \alpha z_o/k_o$. Since we need $z_1 = z_2$, it is necessary that $\alpha = k_o z_2/z_o$ or $\alpha = k_o z_s$, where $z_s = z_2/z_o$. (Note that z_2 is the wave impedance in Medium 2, and z_o is the free-space impedance.)

and

$$\beta = k_o \left(1 - \frac{ik_o}{\sigma z_o}\right)^{\frac{1}{2}} \approx k_o - i\,\frac{k_o^2}{2\sigma z_o} \quad . \tag{8}$$

That is, we have

$$\alpha'' \approx \alpha' \approx k_o^{3/2}\,(2\sigma z_o)^{-\frac{1}{2}} \quad , \tag{9}$$

where

$$k_o = 2\pi/\lambda_o \text{ and } \sigma = 4 \text{ mhos/meter.}$$

If we denote the tilt of the phase front of the surface wave with respect to the interface by θ', it is clear that $\tan\theta' = \alpha'/\beta'$. The values of the parameters α', α'', β', β'', and θ' are tabulated in Table II for a range of frequencies.

The behavior of the $\underline{E}$ field components can be obtained from that of H_y through Maxwell's equations. From

$$\vec{\nabla} \times \vec{H} = -\frac{\partial \vec{D}}{\partial t} = i\omega\varepsilon_o \vec{E} \quad , \quad x > 0$$

we have

$$E_x i\omega\varepsilon_o = -\frac{\partial H_y}{\partial z} \quad , \quad x > 0 \tag{10}$$

and

$$E_z i\omega\varepsilon_o = \frac{\partial H_y}{\partial x} \quad , \quad x > 0 \quad .$$

The power flow along z, per unit width of the surface, is given by

$$P_z = \frac{1}{4}\,\frac{\beta'}{\alpha''}\,\frac{z_o}{k_o}\,AA^* e^{-2\beta'' z} \quad , \tag{11}$$

and the power flow into the surface P_L (due to losses on the surface), per unit area, is given by

Table II

PROPAGATION PARAMETERS FOR A SMOOTH SURFACE--A SLIGHTLY POOR CONDUCTOR

Frequency (MHz)	Parameters					
	λ_o (m)	α' (m^{-1})	α'' (m^{-1})	β' (m^{-1})	β'' (m^{-1})	θ' (degrees)
10	30	0.1745×10^{-2}	0.1745×10^{-2}	0.2093	0.1455×10^{-4}	0.477
1	300	0.522×10^{-4}	0.552×10^{-4}	2.093×10^{-2}	0.1455×10^{-6}	0.1508
0.1	3000	0.1745×10^{-5}	0.1745×10^{-5}	2.093×10^{-3}	0.1455×10^{-8}	0.0477

$$P_L = \frac{1}{4} R_s Z_o AA^* e^{-2\beta''z} \frac{\left(1 - e^{-2\beta''z}\right)}{\beta''}$$

$$\approx \frac{1}{2} R_s Z_o AA^* e^{-2\beta''z} \quad \text{(for small } \beta''\text{)} \quad . \qquad (12)$$

It is clear from the values of θ' given in Table II that at the frequencies of interest the phase front is practically normal to the interface. Stated differently, we have $E_z/E_x \ll 1$.

B. Stochastically, Slightly Rough Surface

The main result of interest to us that has been obtained in Sec. III-A regarding the amplitude of the surface wave (ignoring the phase factors) is

$$H_y \sim e^{-\alpha''x} \quad , \quad x > 0 \quad , \qquad (13)$$

where α'' is seen to be a decay constant. That is, the magnetic field H_y (hence E_x and also E_z) decays with increasing distance from the interface.

In practice, however, the surface of the sea is slightly rough even under "quiet" sea conditions. Let us assume that the roughness is stochastic in character, where the wave heights (or heights of irregularities from the smooth, idealized sea surface) are describable by a probability distribution. We further assume that the maximum height h_{max} of any irregularity is small, $h_{max} \ll \lambda_o$. Note also that for the physical optics approximation to be valid, it is necessary that $dh/dz \ll h/\lambda_o$.

With the above in mind, the results for a smooth surface can be used:

$$\left.\begin{matrix} H_y \\ E_x \\ E_z \end{matrix}\right\} \sim e^{-\alpha''x} \quad , \qquad (14)$$

where α'' is the decay parameter derived for a smooth surface, and x is essentially the instantaneous height (since the speed of light c >>> speed of ocean waves).

Note that if a sensor is located at an average height x_o from the interface, one may write (ignoring the phase factors)

$$H_y \sim e^{-\alpha''(x_o+\tilde{x})} ,$$

where $\tilde{x}$ is the instantaneous wave height (assumed positive but can be negative) measured with respect to the mean height x_o. However, <u>if</u> the instantaneous height of the sensor from the mean "smooth" surface is known, one may write

$$\left.\frac{E_x^{stochastic}}{E_x^{smooth}}\right|_{instantaneous} \sim e^{-\alpha''\left(x^{inst}-x_o\right)} \cdot e^{i\alpha'\left(x^{inst}-x_o\right)} , \qquad (15)$$

where

$$x^{inst} = x_o + \tilde{x}.$$

If $P(\tilde{x})$ denotes the probability density distribution of wave heights, one can write the following expression for $\langle E_x(x)\rangle$, the ensemble average of the x-component of the electric field,

$$\langle E_x(x)\rangle \sim \int_{-\infty}^{\infty} e^{(i\alpha'-\alpha'')(x_o+\tilde{x})} P(\tilde{x})d\tilde{x} , \qquad (16)$$

other dependences of E_x on t and z having been ignored.

We <u>assume</u> below that the wave heights have a Gaussian distribution;* that is, let

---

*In general, it is possible to express other types of distributions in terms of Gaussian distributions and their derivatives, as is done, for instance, in Gram-Charlier series representations.

$$P(x) = \frac{1}{\sqrt{2\pi\sigma_x^2}} \exp\left[-\frac{(x - x_o)^2}{2\sigma_x^2}\right] \quad . \tag{17}$$

Equation (17) implies that $P(\tilde{x})$ is also Gaussian. Note also that

$$\sigma_x^2 = \langle x^2 \rangle - \langle x \rangle^2 \quad .$$

It is clear that any random variation in the height of a sensor will yield a random variation in the power recorded by it. To estimate this variation in power, we proceed as follows.

The power flowing along the z direction is proportional to $[E_x(x)\ E_x^*(x)]$. When $P(\tilde{x})$ is given by Relation (17), we find that

$$\langle |E_x(x)|^2 \rangle = \langle E_x(x) E_x^*(x) \rangle \sim e^{-2\alpha'' x_o} \cdot e^{2(\alpha'')^2 \sigma_x^2} \tag{18a}$$

$$\langle E_x(x) \rangle \sim e^{-\alpha'' x_o}\ e^{-i(\alpha')^2 \sigma_x^2} \tag{18b}$$

(since $\alpha' \approx \alpha''$, in the present approximation),

and

$$\langle E_x^*(x) \rangle = \langle E_x(x) \rangle^* \sim e^{-\alpha'' x_o}\ e^{i(\alpha')^2 \sigma_x^2} \quad . \tag{18c}$$

Hence,

$$\frac{\langle |E_x(x)|^2 \rangle - |\langle E_x(x) \rangle|^2}{|\langle E_x(x) \rangle|^2} = \left[e^{2(\alpha'')^2 \sigma_x^2} - 1\right] \quad . \tag{19}$$

Note that the left-hand side of Eq. (19) is always positive.

Equation (19) has the following interpretation. Because of the random variations of the sea surface, we will observe a random variation* in the power received by a sensor located above that surface.

---

*This may be called a type of scintillation.

By observing the rms value σ_{E_x} of E_x $\left(\sigma^2_{E_x} = \langle |E_x|^2\rangle - |\langle E_x\rangle|^2\right.$, one can deduce the effective value of $\alpha''\sigma_x$. It is clear that, if σ_x is known, α'' can be estimated, and vice versa. We return to this later.

C. Boundary Treated as a Corrugated Surface

Another model that could be employed in the present discussion involves the assumption that the boundary (sea-air interface) could be represented as a periodically corrugated conducting plane (corrugations infinitesimally thin); see Fig. 2. In this idealized model, the corrugations are assumed to represent the sea waves on the interface. Considering again only the TM mode, one may write

$$H_y = \sum_{n=-\infty}^{\infty} A_n \exp\left[i\omega t - \alpha_n x - i\left(\beta + \frac{2\pi n}{L}\right)z\right] \quad , \qquad x > h \quad , \tag{20}$$

where the A_n's are the modal amplitudes.

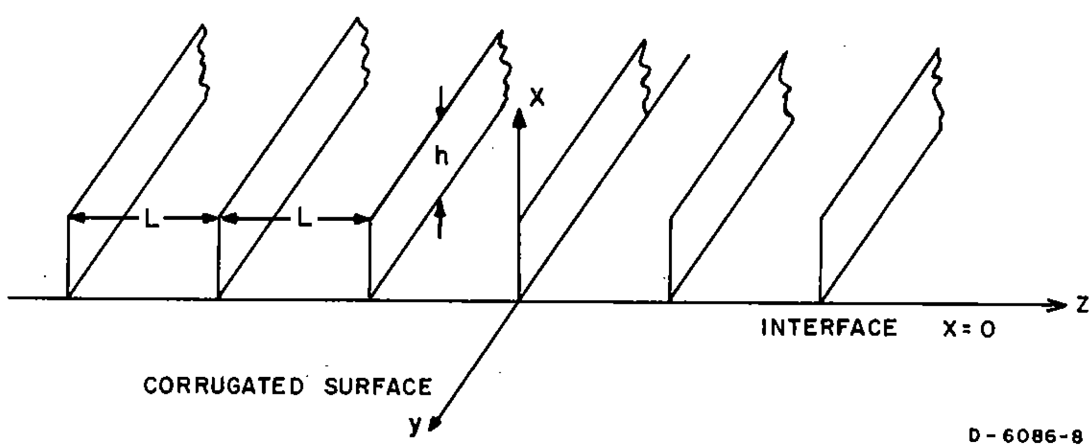

FIG. 2 CORRUGATED SURFACE

One finds from the wave equation that the following condition must be satisfied:

$$\left(\beta + \frac{2\pi n}{L}\right)^2 = k_o^2 + \alpha_n^2 \quad .$$

Note that the representation given by Eq. (20) describes the field for $x > h$ (that is, the region above the crest of the corrugations).

When $h < 0.2\ \lambda_o$,* one can write approximately that

$$\alpha_o \approx k_o \tan k_o h \left(1 - \frac{L \ln 2}{h\pi}\right) \tag{21a}$$

or

$$\alpha_o \approx k_o \tan k_o h \left(1 - \frac{0.22L}{h}\right) \quad . \tag{21b}$$

From Eq. (21a) we observe that a solution for α_o exists only for certain values of k_o and other parameters (α_o is always positive); hence the properties of periodic structures such as the pass and stop bands become evident.

The approximate description of the field component H_y for $x > h$ is given by

$$H_y \approx A\ e^{-\alpha_o (x-h)}\ e^{-i\beta z}\ e^{i\omega t} \quad , \quad x > h \quad . \tag{22}$$

From H_y the other field components can be obtained by employing Maxwell's equations.

Note from Eq. (21) that in the x direction the wave is not attenuated at all (except for losses due to finite conductivity σ):

$$k_o h \left(1 - \frac{0.22L}{h}\right) = n\pi \qquad \text{(no attenuation)} \quad , \tag{23}$$

where n is an integer, $n = 0, 1, 2, \ldots$. Also the attenuation is a maximum--cutoff occurs--whenever

---

*This is the regime of interest to us, since $\lambda_o \approx 30$ meters at a frequency of 10 MHz, and $h < 0.6$ meter under reasonably quiet sea conditions.

$$k_o h\left(1 - \frac{0.22L}{h}\right) = (2n + 1)\frac{\pi}{2} \qquad \text{(cutoff)} \quad , \tag{24}$$

where

$$n = 0, 1, 2, \ldots .$$

The expression for P_z, the power flow along the z direction per unit width along the y direction, is found to be

$$P_z = \frac{AA^*\beta z_o}{4k_o\alpha_o} \quad , \tag{25}$$

and the power loss per unit width of one corrugation P_L is given by

$$P_L = \frac{1}{2} R_s z_o AA^* \sec^2 k_o h\left(L + h + \frac{\sin 2k_o h}{2k_o}\right) \quad . \tag{26}$$

One can also write an expression for the attenuation constant β_L, a measure of the power loss per meter in the z direction, as

$$\beta_L = \frac{P_L}{2LP_z} = \frac{R_s\alpha_o k_o[L + h + (\sin 2k_o h)/2k_o]}{\beta_L \cos^2 k_o h} \quad \text{nepers/meter} \quad . \tag{27}$$

To obtain low attenuation, the surface wave should be loosely bound to the surface, that is, α_o should be small.

Note also that, if the wave heights are randomly distributed according to some probability distribution such as P(h), then by employing a procedure similar to that given in Sec. III-B, one could obtain expressions for mean square deviations of the appropriate electric magnetic field components or both. The results would show that the cutoff and pass bands are not as well defined as Eqs. (23) and (24) indicate.*

---

*Similar considerations apply for random variations in L.

IV SCATTERED FIELDS NEAR AN EXTENDED SOURCE

Scattering may appreciably modify the signal from an extended source. Consider a semicircular cylindrical dipole sheet of charge suddenly created above a conducting plane surface, as shown in Fig. 3.

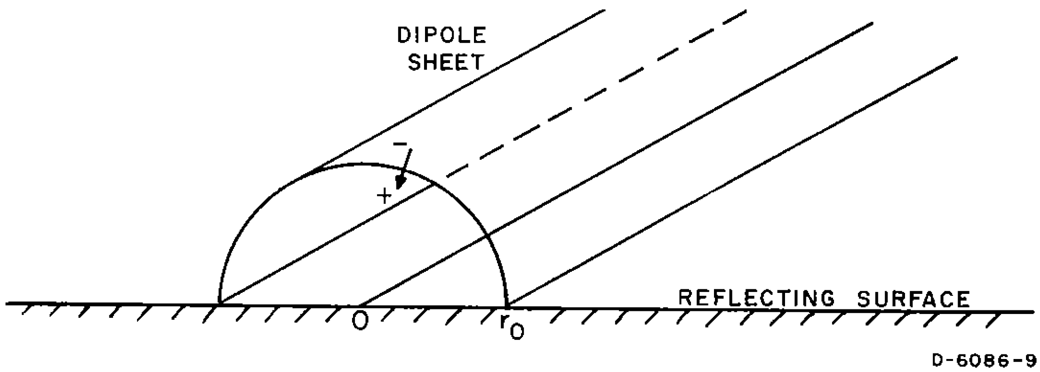

FIG. 3 EXTENDED SOURCE MODEL

The source geometry in the x-y plane, normal to the cylinder axis along z, is shown in Fig. 4. The dipole sheet is created at a time $t_o = t + r_o/c$, where t = 0 is the time at which the ionizing photons are emitted at the cylinder axis, r_o is the radius of the cylinder, and

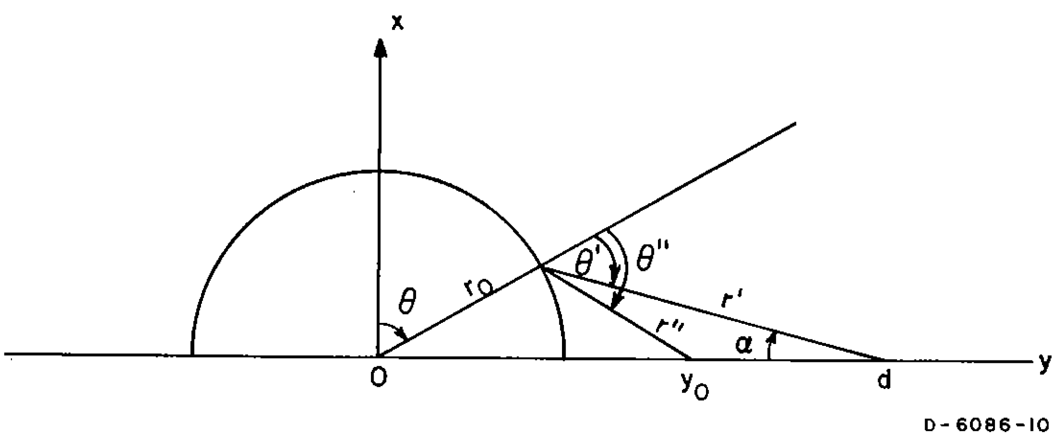

FIG. 4 EXTENDED SOURCE GEOMETRY

c is the speed of light. A dipole element at θ can be observed at d, on the conducting plane surface, only for $ct > r_o + r'$, where r' is the distance from the dipole element to d.

The quasi-static field at d at time t can be written

$$\underline{E}\,(d,t) = \int_{\theta_o(d,t)}^{\pi/2} \underline{E}_d^s\,(d) \quad r_o\, d\theta \quad , \tag{28}$$

where E_d^s is the static field of a constant line-dipole charge distribution above the conducting plane, and $\theta_o(d,t)$ is the minimum θ for which the charge created at t_o can be observed at (d,t). The factor $r_o d\theta$ is an element of arc on the surface of the cylinder.

The static electric field of a line dipole source is

$$\underline{E}(\underline{r}) = \frac{\sigma d\ell}{2\pi\epsilon_o r^2} \left(\cos\,\theta'\hat{\imath}_r + \sin\,\theta'\hat{\imath}_{\theta'}\right) \quad , \tag{29}$$

where $\sigma d\ell$ is the dipole strength per unit length, r the distance from the dipole axis, and θ' the angle of $\underline{r}$ to the plane of the dipole strip. In the source geometry of Fig. 4, Eqs. (28) and (29) yield, for the vertical (x) component of the electric field at (x,y) = (0,d),

$$E_x(d,t) = \frac{\sigma d\ell}{\pi\epsilon_o} \int_{\theta_o(t)}^{\pi/2} d\theta r_o \, \frac{(\sin\,\alpha\,\cos\,\theta' + \cos\,\alpha\,\sin\,\theta')}{r'^2} \quad , \tag{30}$$

where $\sigma d\ell$ now represents the strength per unit area of the surface-dipole layer, and twice the E_x given by Eq. (29) has been used to include the image of the charge distribution in the conducting plane. After some trigonometric manipulations, the integrand in Eq. (30) can be represented solely in terms of the integration variable θ:

$$E_x(d,t) = \frac{\sigma d\ell \; r_o\left(d^2 - r_o^2\right)}{\pi\epsilon_o}\int_{\theta_o(t)}^{\pi/2} d\theta \; \frac{\cos\theta}{\left[d^2 + r_o^2 - 2\, r_o d \sin\theta\right]^2} \quad . \qquad (31)$$

Equation (31) integrates readily to

$$E_x(d,t) = \frac{\sigma d\ell \; r_o(d + r_o)[1 - \sin\theta_o(t)]}{\pi\epsilon_o(d - r_o)\left[d^2 + r_o^2 - 2\, r_o d \sin\theta_o(t)\right]} \quad . \qquad (32)$$

Finally, the relation $ct = r_o + r'$ yields

$$\sin\theta_o(t) = \frac{d^2 + r_o^2 - (ct - r_o)^2}{2\, r_o d} \quad , \qquad (33)$$

which, when used in Eq. (32), gives

$$E_x(d,t) = \frac{\sigma d\ell}{\pi\epsilon_o d(d - r_o)}\begin{cases} 0 & ct \leq d \\ \dfrac{(d + r_o)[(ct - r_o)^2 - (d - r_o)^2]}{2\, r_o(ct - r_o)^2} & d \leq ct \end{cases} \quad . \qquad (34)$$

Scattering elements, located between r_o and the observation point d, may be treated to first approximation simply as reflecting surfaces. They produce a contribution to the field at d equal to some fraction of the field present at the scatterer at the retarded time for propagation between the scatterer and d. The amplitude of the scattered field depends primarily upon the shape of the scatterer and its size relative to the wavelengths of interest. An accurate determination of the scattering coefficients, with a full treatment of the radiation problem, has not been pursued here. The buildup of the quasi-static field of the charge distribution has been calculated as an example (see Chap. V), but the radiation field has not been calculated. A rough estimate of the value of the scattering coefficient for the radiation field could be obtained by comparing the area of the scattering surface with that of the first Fresnel zone on an infinite plane surface tangent to the scattering surface at the specular reflection point.

The total field is represented by a sum of terms of the form of Eq. (34):

$$E_x(d,t) = \sum_{i=0}^{n} E_x^i(d,t) \quad , \qquad (35)$$

where

$$E_x^i(d,t) = \alpha_i E_x^i\left(y_i, t - \frac{d - y_i}{c}\right) \quad , \qquad (36)$$

with the primary field at d represented by i = 0, with $\alpha_o = 1$, and with the scattering contribution represented by the remaining terms, with α_i being the scattering coefficient for the scatterer at y_i.

V DISCUSSION AND CONCLUSIONS

Physical feeling for the attenuation of surface waves normal to the sea-air interface can be obtained from the following.

From Table II, we observe that the attenuation constant (normal to the interface) is a small quantity, even at 10 MHz. That is, unless the detector is located at a height of tens of meters from the surface, one will not be able to observe any noticeable change in (a component of) field amplitude at the elevated sensor from the corresponding (component of) field amplitude at the interface. Note also that the attenuation constant β'' along the direction of propagation in the plane of the interface is very small, and the phase front of the surface wave is very nearly normal to the interface.

From Eq. (19) we observe that the rms deviation of a field (component)--owing to the sea surface being random--is a function of α'', the decay rate of the field normal to the surface, and of σ_x, the rms deviation of the wave heights. Again, because under quiet sea conditions σ_x is a small quantity, it is extremely difficult to observe by experimental measurements the effect of random irregularities of sea surface on surface wave propagation, at the frequencies of interest here. For a wave height of 0.5m, for example, $\langle x^2 \rangle - \langle x \rangle^2$ is approximately 0.03 m^2 (the mean square deviation of a sinusoidal surface from the mean height). This value and that of 1.745×10^{-3} for α'' at 10 MHz from Table II yield a value, from Eq. (19), of 1.906×10^{-7} for the mean square variation of the field relative to the average field. At lower frequencies, the variation would be smaller, since α'' decreases with decreasing frequency.

For the case of the corrugated surface model, let us consider the following example.

Assume:

Frequency of EM wave = 10 MHz

Height h of the wave (corrugation) = 0.5 meter.

(This value of h represents fairly quiet sea conditions.)

For a surface wave to exist, we require that α_o be positive. Recall that

$$\alpha_o = k_o \tan k_o h \left(1 - \frac{0.22L}{h}\right) \quad . \qquad (21b)$$

Since k_o is always positive, we find that we need here

$$\left.\begin{array}{l} 0 < \theta < \frac{\pi}{2} \\ \text{or,} \\ -(2n + 1)\pi < \theta < -\left(2n\pi + \frac{\pi}{2}\right) \quad , \\ \text{where} \\ \theta = k_o h \left(1 - \frac{0.22L}{h}\right) \quad . \end{array}\right\} \qquad (37)$$

In this example, we find that surface wave propagation occurs when

$$0 < L < 2.7 \quad \text{meters}$$

or

$$[n(136) + 36.4] < L < [n(136) + 70.5] \quad \text{meters} \quad , \qquad (38)$$

where

$$n = 0, 1, 2, \ldots .$$

The first cutoff occurs when L = 36.5 meters.

The behavior of α_o as a function of frequency f (with h and L fixed) and the behavior of α_o as a function of L (with h and f fixed) is shown in Figs. 5 and 6, respectively. Since we are dealing with a periodic structure, the general behavior of α_o repeats itself periodically.

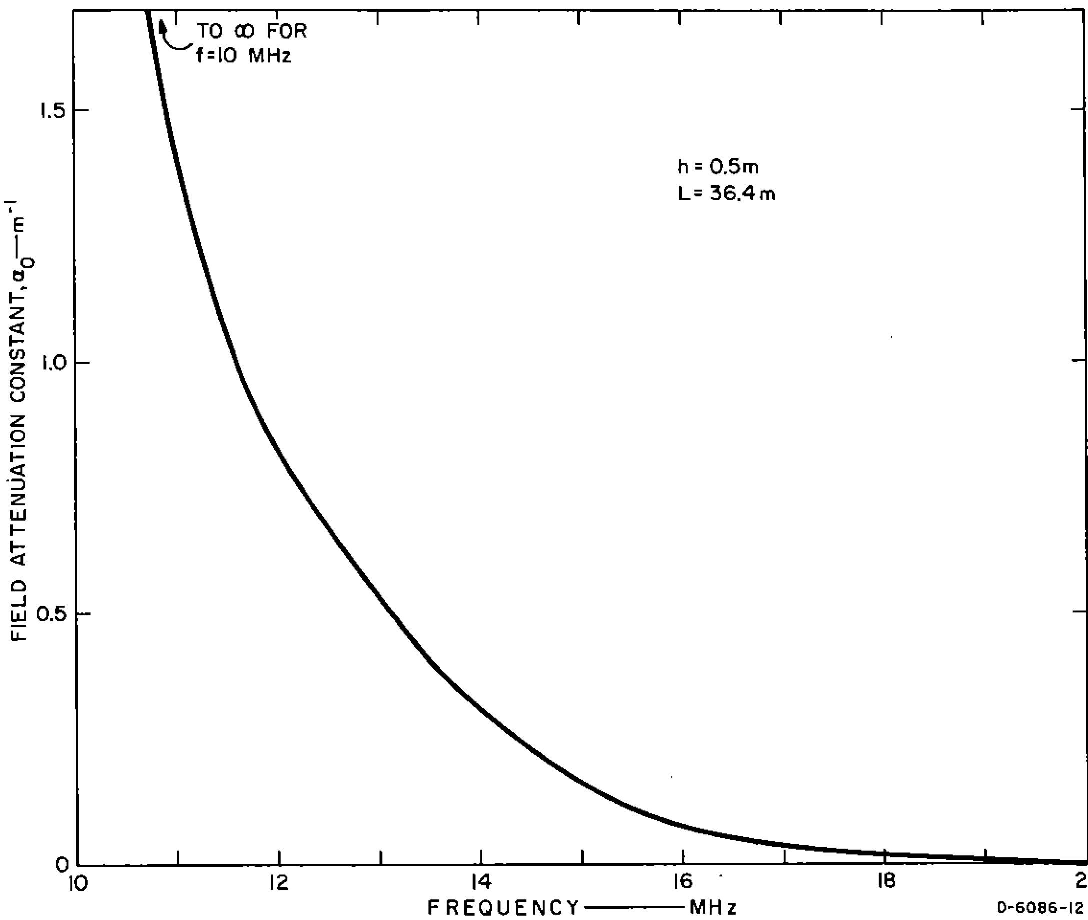

FIG. 5 α_0 AS A FUNCTION OF f WITH h AND L CONSTANT

Figures 5 and 6 indicate that in principle (when the surface is represented by a periodically corrugated surface), one would observe the stop and pass bands. However, since the sea surface is not as well defined as in the case of the assumed model, it would be extremely difficult to correlate any experimental measurements with theoretical predictions.

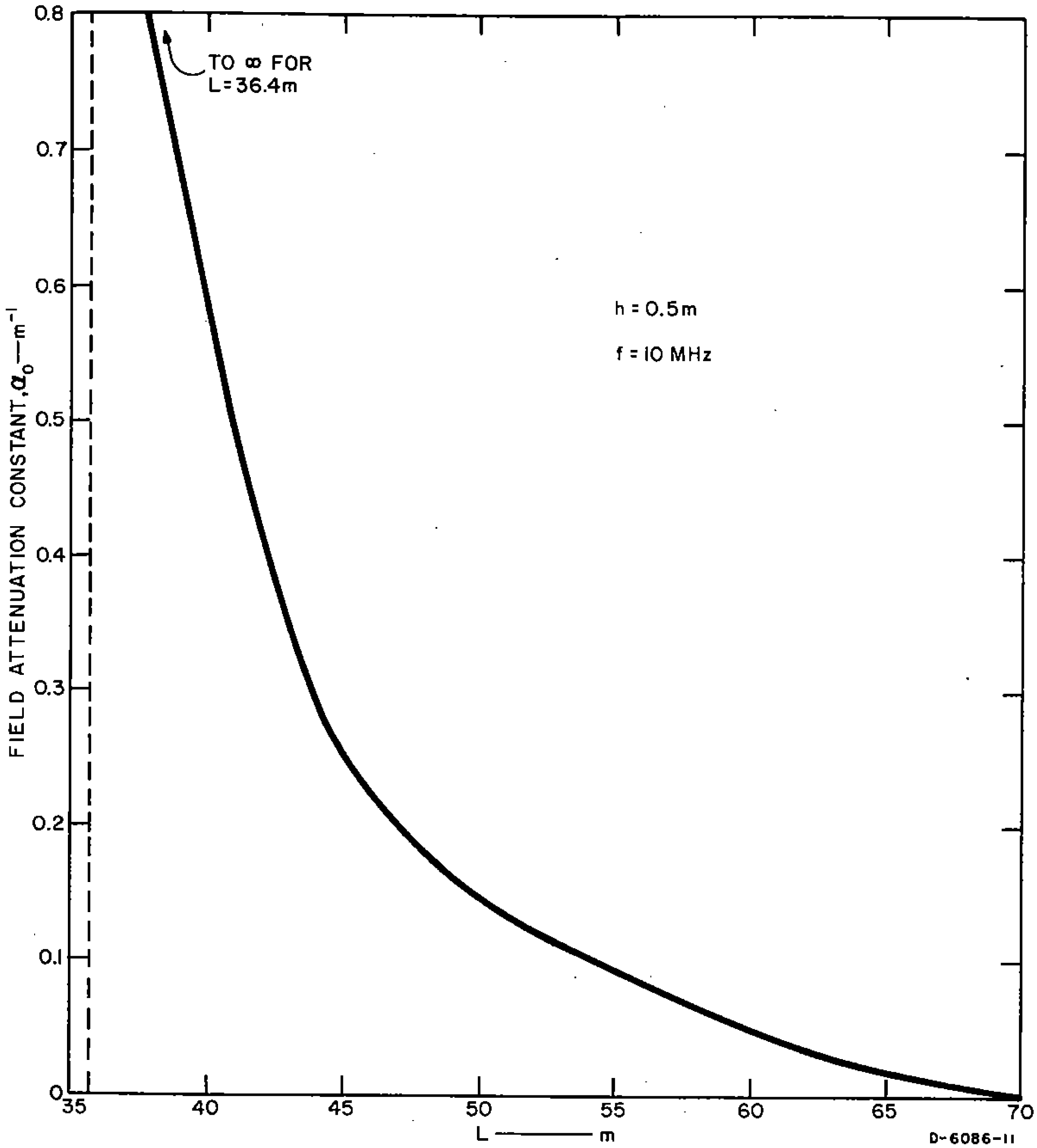

FIG. 6 α_0 AS A FUNCTION OF L WITH h AND f CONSTANT

Finally, note that the effects on surface wave propagation of moisture (dampness) due to temperature gradients (near the surface) and of spray due to winds have not been considered in the present treatment.

Regarding the effects of scattering upon the signal from an extended source, the model developed in Chap. IV exhibits some interesting features. The shorter the distance from the source, the more rapid is the signal rise at early times. Equation (33) indicates that this behavior results, in part, because the different elements of the surface become observable at a faster rate at the shorter distance. Thus, the signal scattered from some point between the source and the observer has a faster rise at early times than does the direct signal.

This characteristic of a faster rising signal at shorter distances is enhanced if the charge distribution resides at the surface of a conducting cylinder, rather than in empty space. In this case, a portion of the charge distribution (that for which $\theta' > \pi/2$ in Fig. 4) is shielded from observation by the intervening cylinder. Thus, the time required for $\theta'(t)$ to change from 0 to $\pi/2$ is characteristic of the rise time of the observed field. This time interval is given by

$$c\ \Delta t = c\left[t\left(\theta' = \frac{\pi}{2}\right) - t\left(\theta' = 0\right)\right]$$

$$= \left[\left(d^2 - r_o^2\right)^{\frac{1}{2}} + r_o\right] - d \quad . \tag{39}$$

The shielding action of the cylinder is greater at the higher frequencies, where diffraction of the fields around it is less.

Now consider scattering from some perturbation of the surface at $(0,y_o)$, $r_o < y_o < d$. The rise time at d of the scattered field from y_o is determined by the time at which the shielding action of the cylinder becomes evident at y_o rather than by the time at which this action becomes evident at d. Thus, this rise time is characterized by the interval between $\theta''(t) = 0$ and $\theta''(t) = \pi/2$. This time interval is given by

$$c\ \Delta t_s = \left[\left(y_o^2 - r_o^2\right)^{\frac{1}{2}} + r_o\right] + (d - y_o) - d$$

$$= \left[\left(y_o^2 - r_o^2\right)^{\frac{1}{2}} + r_o\right] - d \quad . \qquad (40)$$

Comparison of Eqs. (39) and (40) reveals that $\Delta t_s < \Delta t$. The contribution from a given dipole element of the source arrives at (0,d) later via the scattered path than via the direct path. However, some source elements are visible via the direct path that have greater propagation delays (up to Δt) than does the element at $\theta'' = \pi/2$, that has the maximum delay (Δt_s) via the scattered paths.

Values of Δt_s are given in Table III for r_o = 1 and 2 km and a range of values of y_o between 2 and 10 km. The difference in characteristic times between the shorter and the longer distances in Table III is large enough to suggest that the form of the observed signal can be appreciably altered by scattering of sufficient amplitude.

Table III

RISE TIME OF SIGNAL FROM AN EXTENDED SOURCE

y_o (km)	Δt_s (μs)	
	r_o = 1 km	r_o = 2 km
2	2.44	--
3	2.77	4.13
5	3.00	5.27
7	3.10	5.70
10	3.17	6.00

Equations (34) and (35) have been used to calculate the quasi-static field at d = 5 km from a conducting cylindrical source of 1-km radius with a series of scatterers at various distances between r_o and d. As noted previously, the scattering is treated only roughly in these examples, by simply taking some fraction of the field present at the scatterer [at the retarded time $(d - y_o)/c$] to represent the scattered field at d. Each of the scatterers then contributes a term of the form of Eq. (34) to the total field.

Until the time at which $\theta' = \pi/2$ is reached Eq. (34) is a reasonable representation of the quasi-static field. After this time, it presents difficulties however, since it fails to represent properly the contribution made to the signal at d by dipole elements beyond $\theta' = \pi/2$, which are partially shielded by the conducting cylinder. For angles $\theta' > \pi/2$, the field has been held constant at its value at $\theta' = \pi/2$ in the calculations made here. This is essentially a high-frequency approximation, and it overemphasizes the effect of the conducting cylinder upon the lower-frequency fields.* Thus, the rate of change of the field from a given scatterer can be expected to show a rapid decrease at $\theta'' = \pi/2$ but not to zero, as assumed here. This approximation somewhat exaggerates, therefore, the distortion of the signal by the scattering.

Figure 7 illustrates the fields calculated for a series of scatterers spaced uniformly at 0.5-km intervals between $r_o = 1$ km and $d = 5$ km, with a linearly increasing scattering coefficient from 0.04 at $y_1 = 1.5$ km to 0.1 at $y_7 = 4.5$ km and with exponentially increasing coefficient (factor of 2 per 0.5-km interval) from 0.003125 at $y_1 = 1.5$ km to 0.2 at $y_7 = 4.5$ km. The primary-field term ($i = 0$) is also plotted separately.

The plots, which are of the quantity $\epsilon_o \pi E_x(d,t)/\sigma d \ell r_o$, have been normalized to facilitate comparison of the rise rates of the three signals. The final amplitudes reached are $5 \times 10^{-8} m^{-2}$, $9.15 \times 10^{-8} m^{-2}$, and $1.79 \times 10^{-7} m^{-2}$ for the primary field, the exponentially increasing scattering-coefficient case, and the linearly increasing scattering-coefficient case, respectively. The latter of the two scattering cases has the greater contribution from scatterers which are much nearer the source than is the observation point; this condition yields both the

*Note that in Eq. (28) the ultimate static field is exactly given by the integral over θ from $-\pi/2$ to $\pi/2$.

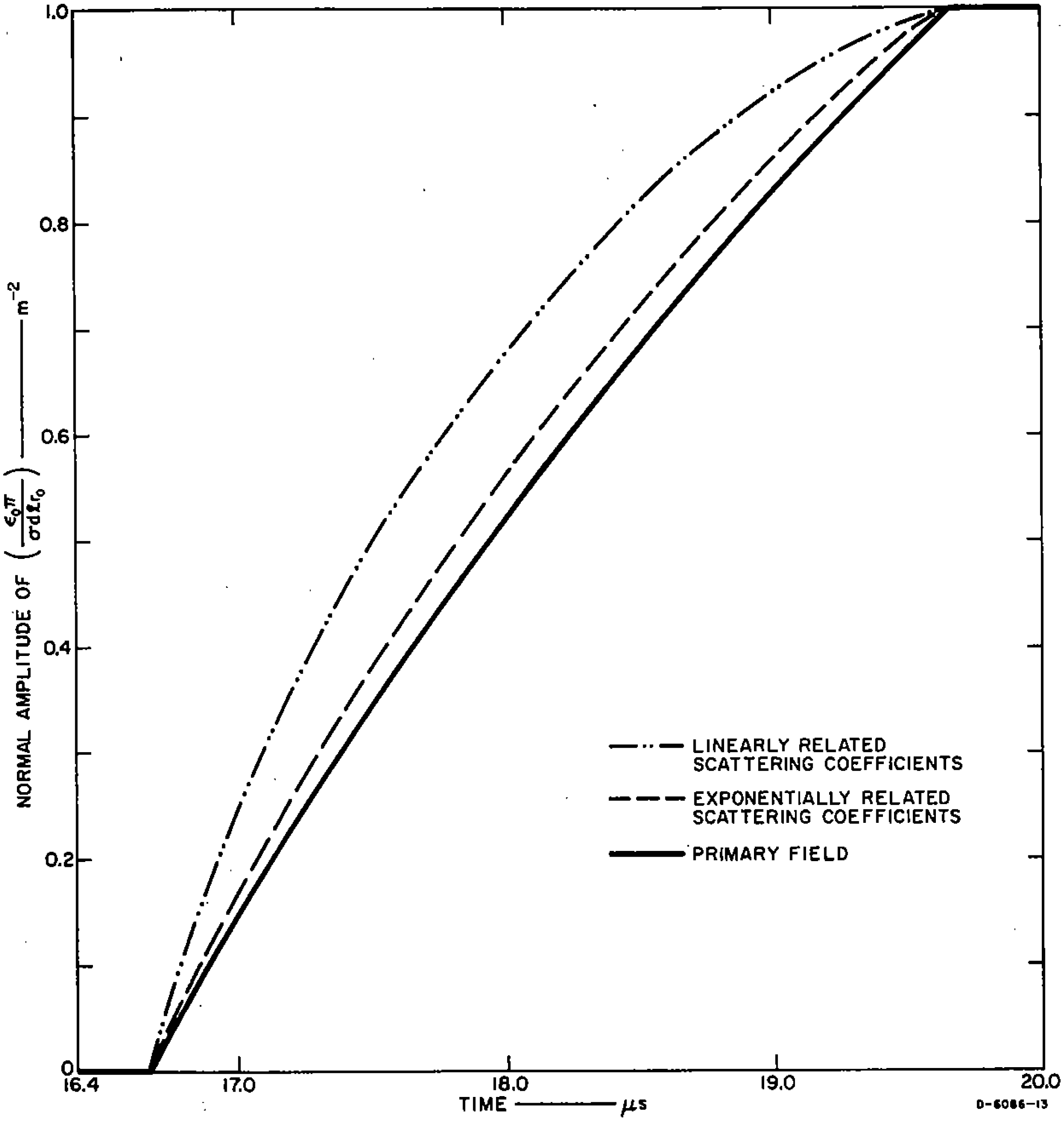

FIG. 7 QUASI-STATIC FIELD FOR A STEP-FUNCTION CYLINDRICAL DIPOLE SHEET

faster rise and the larger amplitude of this case relative to the other. An increase in rise rate relative to that of the primary field is evident in both cases, however.

Note that the scattered field contributions at 5 km were calculated by multiplying the scattering coefficients and the fields at the scattering point, with no further decrease in field amplitude between this point and 5 km. Thus, these calculations involve stronger scattering, especially from the scatterers near the source, than may be suggested by the values of the coefficients used.

The mean square variation of the field from its mean value could be estimated for a stochastically rough surface using the model described in Chap. IV. However, this development seems best deferred until the model has received a more precise treatment than that presented here.

VI GENERAL REFERENCES

J. A. Stratton, Electromagnetic Theory (McGraw-Hill Book Company, Inc., New York, New York, 1941).

R. E. Collin, Field Theory of Guided Waves (McGraw-Hill Book Company, Inc., New York, New York, 1960).

H. Cramer, Mathematical Methods of Statistics (Princeton University Press, Princeton, New Jersey, 1946).